

SU 64-5

33p.

Ns B-233-62  
N64-19615 X  
CODE-1  
NASA CR-53829



OTS PRICE

XEROX

MICROFILM

\$ 3.60 ph  
\$ 4.19 mg.

UNPUBLISHED PRELIMINARY DATA

Department of Physics and Astronomy  
**STATE UNIVERSITY OF IOWA**

Iowa City, Iowa

RC #1

CNASCAR

-----; SUI-64-5)  
OTS:

T

Large Diurnal Variations of Geomagnetically  
Trapped and of Precipitated Electrons  
Observed at Low Altitudes *te*

by

L. A. Frank, J. A. Van Allen,  
and J. D. Craven *\*\*\* mar. 1964 33 p*  
*reger*

March 1964

1362243

Department of Physics and Astronomy  
Iowa State University of Iowa  
Iowa City, Iowa

\* Research supported in part by the Office of Naval Research under  
contract N9onr-93803) and by the National Aeronautics and Space  
Administration under grant NSG-233-62;

(NASA

\*\* Graduate research fellow of the National Aeronautics and Space  
Administration.

## ABSTRACT

19615

A large, similar diurnal variation of the intensities of geomagnetically trapped and of precipitated electrons is observed in data obtained with the low-altitude satellite Injun III over the period December 1962 to September 1963. The northern limit of detectable electron ( $E \geq 40$  keV) intensities was at  $L \sim 20$  ( $\lambda \sim 77^\circ$ ) at local noon and at  $L \sim 8$  ( $\lambda \sim 69^\circ$ ) at local midnight. Several polar plots of the median intensities of electrons as a function of local time and the shell parameter  $L$  (and  $\lambda = \arccos L^{-1/2}$ ) are displayed. A local acceleration mechanism for electrons ( $E \geq 40$  keV) on the sunward side of the magnetosphere is suggested in this preliminary study by an apparent maximum of precipitated electron intensities near local noon at  $L \sim 8$ . The diurnal effect (a factor of the order of 100 or greater) begins abruptly at  $L \sim 8$  and extends to all higher  $L$  shells; the local time dependence of the median electron intensities is more or less symmetrical about the noon-midnight meridian but may be more nearly symmetrical about a meridian of  $\sim 11:00$  ( $\pm 2$  hours) beyond  $L \sim 10$ .

*Author*  
*201404*

# I. INTRODUCTION

By the use of earth satellites and space probes, it has become possible to observe, in situ, departures from rotational symmetry of the earth's magnetic field and of the charged particle distributions therein, which have been previously suggested by ground-based observations of upper atmospheric phenomena [cf. Axford and Hines, 1961]. Charged particle measurements near the geomagnetic equatorial plane at large radial distances from the center of the earth with Explorers XII and XIV [Frank, Van Allen, and Macagno, 1963] have shown a strong dependence of the electron intensities on the angle from the earth-to-sun line; the outermost limit of large electron intensities is  $\sim 10 R_E$  at local noon and  $\sim 8 R_E$  at local midnight and beyond  $16 R_E$  at local morning. Also a significant diurnal variation of the intensities of trapped electrons has been observed at low altitudes and high latitudes with Injun I [O'Brien, 1963]; the northern limit of trapped electrons at 1,000 km altitude was at  $\sim 75^\circ$  geomagnetic latitude at local noon and only  $\sim 69^\circ$  at local midnight. Investigations of this effect in terms of distortion of the geomagnetic field by the solar wind have been attempted [Akasofu, 1963; Hones, 1963]. Ground-based experimental

researches such as auroral riometer measurements [Little and Leinbach, 1958; Pasler, 1963] and visual auroral studies [cf. Davis and DeWitt, 1963] have found significant local time variations of these phenomena of the upper atmosphere. If in turn these phenomena are attributable to the downflux of corpuscular energy from the magnetosphere surrounding the earth, similar, large diurnal effects should be expected in the precipitated charged particle fluxes. Precipitation of electrons into the atmosphere has previously been observed by direct detection with Injun I [O'Brien, 1962]. Further, from the gross spatial and temporal characteristics of the charged particle distributions within the near and distant magnetosphere, important information concerning local acceleration mechanisms can be obtained.

A preliminary survey of the diurnal variations of trapped and of precipitated electrons at high latitudes using data from the low-altitude satellite Injun III for the period December 1962 through September 1963 is given in the following presentation.

## II. EXPERIMENTAL EQUIPMENT

The Injun III satellite which was designed and constructed at the State University of Iowa was launched on December 13, 1962 into an orbit with apogee altitude of 2795 km, perigee altitude of 237 km, an orbital inclination of  $70.4^\circ$ , and a period of 1.94 hours. A description of the satellite equipment is given by O'Brien, Laughlin, and Gurnett [1964]; we shall discuss only those details which are of pertinence to the present investigation. Injun III was magnetically aligned with respect to the local magnetic field by means of an on-board magnet, and the fields of view of the charged particle detectors were designed to utilize this magnetic orientation in order to distinguish between the geomagnetically trapped and the precipitated corpuscular radiation. On-board magnetometers allowed a verification of the proper orientation of the satellite with respect to the local geomagnetic field direction. A graphical summary of the local times for the satellite over North America for each month of observations used in the present analysis is given in Figure 1. Since data are available over the period December 1962 through the middle of September 1963 the precession of the orbital plane allowed us to eventually sample all local times.

Real-time telemetry for Injun III was received by stations throughout the world, but predominantly in North America. The magnetic tapes were then sent to SUI where decoding and merging with an ephemeris supplied by the Goddard Space Flight Center of NASA were performed.

Two charged particle detectors of the Injun III complement are of primary interest in this preliminary survey of diurnal effects: (a) an unshielded Anton type 213 thin-windowed ( $1.2 \text{ mg/cm}^2$  mica) Geiger-Mueller tube with a conical field of view of half-angle  $43^\circ$  whose axis was directed upward along the local magnetic field vector when the satellite was in the northern hemisphere and was oriented properly, and (b) a similar detector with a conical field of view of half angle  $13^\circ$  whose axis was directed  $90^\circ$  to the local magnetic field vector. The former detector measures the intensity of electrons precipitated into the atmosphere with a unidirectional geometric factor of  $0.6 \times 10^{-2} \text{ cm}^2 \text{ sr}$  and the latter detector measures the intensity of trapped electrons with a unidirectional geometric factor of  $1.5 \times 10^{-2} \text{ cm}^2 \text{ sr}$ . Both detectors have electron thresholds of 40 keV [cf. Frank and Van Allen, 1963] and proton energy thresholds of 500 keV. Identification of the responses of these detectors at  $L \gtrsim 4.0$  as those due to electrons ( $E \gtrsim 40 \text{ keV}$ ) rather than due to protons

( $E \geq 500$  keV) is provided by the p-n junction detectors on Injun III which simultaneously measure the intensities and energy spectrum of protons ( $700 \text{ keV} \leq E \leq 100 \text{ MeV}$ ) (courtesy of C. Bostrom and G. Pieper of the Applied Physics Laboratory, Johns Hopkins University). Less than 2% of the data was contaminated by small solar proton events. The Geiger-Mueller tubes are also sensitive to soft solar x-rays (efficiency  $\sim 10^{-2}$  to  $10^{-1}$  over the range of 4 to  $12 \text{ \AA}$ ); the infrequent periods of contamination by soft solar x-rays are identified by the characteristic counting rate peak as the corresponding detector's field of view scans the sun and by verifying that the sun was within the detector's field of view by means of on-board light-sensitive devices. The median counting rates of both of the above detectors were in the linear region of detector response as a function of incident electron intensity and uncertainties in corrections for the dead-time of these instruments for above-median counting rates did not have any influence on the median rates, of course.



### III. ANALYSIS OF DATA

The approach of this preliminary investigation of the gross diurnal variations of electron ( $E \geq 40$  keV) intensities using Injun III data is straightforward. Over 700 passes of data at  $L \gtrsim 4.0$  were available for analysis; a short synopsis of these passes as to station, hemisphere, and month is given in Table I. The data are predominantly from North American stations ( $\sim 90\%$ ) and hence the results of the present analysis pertain especially to this region. The data were ordered with respect to the B and L parameters [McIlwain, 1961] and were assigned to the appropriate local time at the point of observation. For a chosen value of L, the data were grouped according to ranges of B and plotted as a function of local time. Eight-second averages of the detector counting rates were used; only one data point per pass was assigned to a given L value and no selections of the data according to  $K_p$  or season were made in this preliminary investigation. Only northern latitude passes were used to study the diurnal variations of electron precipitation (the corresponding detector looks downward, toward the earth, in the southern hemisphere); both northern and southern hemisphere passes were used in the study of trapped electron intensities although the number of southern passes is comparatively small (see Table I).

TABLE I

Summary of Satellite Passes Used  
in the Present Investigation

Total Passes .....	725
Northern Hemisphere .....	664
Southern Hemisphere .....	61
December 1962 .....	42
January 1963 .....	86
February .....	73
March .....	47
April .....	67
May .....	112
June .....	140
July .....	122
September .....	36
Percentage of Passes by Station:	
Iowa City (SUI) .....	47%
Prince Albert (Canada) .....	26%
College (Alaska) .....	11%
Woomera (Australia) .....	8%
St. Johns (Canada) .....	5%
Other .....	3%

## IV. PRESENTATION OF DATA

The response of the trapped electron ( $E \geq 40$  keV) detector for various values of  $L$  as a function of local time is displayed in Figures 2 and 3. Each data point for a given value of  $L$  represents a measurement for an individual satellite pass. The various symbols in the above graphs represent ranges of  $B$  in order to evaluate the relative importance of this parameter with respect to temporal variations and diurnal effects; these ranges are tabulated in the respective figure captions. The large scatter of the data points at a given local time and  $L$  is seen to be due to true temporal variations of the electron intensities and not to  $B$  dependence. For  $L = 4$  and  $7$  (Figure 2) there is no significant dependence on local time of the median intensities indicated by the solid line segments; the upper and lower dotted line segments show the counting rates above which and below which, respectively, one-fourth of the data points fall. At  $L = 8.5$  the character of the median intensity as a function of local time changes strikingly, with a maximum at approximately local noon and a minimum at local midnight. The noon/midnight ratio is of the order of 100. (If the detector counting rate is 1 count/second or less, the datum is plotted as 1 count/second and hence represents the threshold response.) This large

diurnal variation continues for all higher L values shown in Figures 2 and 3. In Figure 4 is plotted the median response of the trapped electron ( $E \geq 40$  keV) detector as a function of L for a few selected local times to emphasize and summarize the character of the diurnal effect. (The invariant latitude  $\Lambda = \arccos L^{-1/2}$  is used in several of the following graphs displayed in the present investigation and is within  $\sim 2^\circ$  of being equal to the geomagnetic latitude  $\lambda$  over North America.) Median omnidirectional intensity contours in the L-local time coordinate system are summarized in Figure 5 in order to exhibit the gross diurnal features of Figures 2 and 3 in another way. The median omnidirectional intensities of electrons were computed from the median responses of the respective unidirectional detectors by assuming that the electron fluxes were isotropic over the detectors' fields of view and by assuming an altitude of  $\sim 1500$  km to calculate the trapping and dumping cones; the uncertainty in the resulting omnidirectional intensities due to imperfections of the above assumptions is believed to not exceed a factor of 2 or 3 in absolute values. The uncertainty in relative values is trivial. The limit of detectable trapped electron intensities is at  $L \sim 8$  at local midnight and  $L \sim 20$  at local noon. At  $L = 9$ , the median electron intensity at local noon is

$\sim 6 \times 10^5 \text{ (cm}^2 \text{ sec)}^{-1}$  and at local midnight is far less than  $3 \times 10^3 \text{ (cm}^2 \text{ sec)}^{-1}$ . The iso-intensity contours show an approximate symmetry with respect to the noon-midnight meridian but do appear more nearly symmetrical about a meridian of  $\sim 11:00$  local time beyond  $L \sim 10$ . An alternative graph of the median intensities of trapped electrons ( $E \geq 40 \text{ keV}$ ) referred to the  $\Lambda$ -local time coordinate system is shown in Figure 6; the limit of detectable intensities of electrons was at  $\Lambda \sim 69^\circ$  at local midnight and  $\Lambda \sim 77^\circ$  at local noon over North America.

A similar analysis has been performed for the intensities of electrons precipitated into the upper atmosphere and the response of the corresponding detector as a function of local time is displayed in Figures 7 and 8. These median counting rates also show the onset of a diurnal variation of two orders of magnitude between  $L = 7$  and  $8.5$ . The depression of the median at  $L = 4.0$  from local midnight to  $8:00$  may be due to a B dependence of the electron intensities but no interpretation of this observation is given here. A few local times have been selected and the median counting rate plotted as a function of  $L$  in Figure 9, which displays the rapid decrease at  $L \sim 8$  on the midnight meridian and significant precipitated electron

intensities to  $L \gtrsim 20$  on the noon meridian as in the case of the trapped electron intensities discussed previously. Again the median electron intensities have been summarized in a  $L$ -local time coordinate system in Figure 10. There is a broad minimum during local night and an apparent maximum during local day at  $\sim 11:00$  and  $L \sim 8$ . The northern limit of detectable electron precipitation is at  $L \sim 8$  at local midnight and  $L \sim 20$  at local noon; this northern limit is at  $\lambda \sim 69^\circ$  at local midnight and  $\lambda \sim 77^\circ$  at local noon (see Figure 11) over North America.

## V. DISCUSSION

A large diurnal variation of the intensities of trapped and of precipitated electrons observed at low altitudes with Injun III is reported in this preliminary investigation. The high latitude limits of detectable trapped and of detectable precipitated electrons ( $E \geq 40$  keV) intensities are similar and are at  $L \sim 8$  ( $\lambda \sim 69^\circ$ ) near local midnight and at  $L \sim 20$  ( $\lambda \sim 77^\circ$ ) near local noon. There is some tendency for the distribution of precipitated electrons to extend to higher values of  $L$ , at a low intensity level, during mid-day (compare Figures 4 and 7). The present finding of a large diurnal variation in the intensities of trapped electrons is in agreement with a study of individual passes at low altitudes with Injun I [O'Brien, 1963]; however, the accompanying finding of a large diurnal variation of the intensities of electrons ( $E \geq 40$  keV) precipitated into the atmosphere is in disagreement with O'Brien [1964] who concluded tentatively in an early report that no local time dependence of precipitated (dumped) electron intensities is evident in the Injun III data. The iso-intensity contours of both trapped and precipitated electrons (see Figures 5 and 10) are approximately symmetrical with respect to the noon-midnight meridian but at  $L \gtrsim 10$  this symmetry appears to be displaced to a meridian of  $\sim 11:00$ .

An apparent maximum of the intensities of precipitated electrons ( $E \geq 40$  keV) occurs at approximately local noon ( $\sim 9:00$  to  $13:00$ ) at  $L \sim 8$  where the electron intensity is  $\sim 5 \times 10^4$  ( $\text{cm}^2 \text{ sec}^{-1}$ ); this maximum strongly indicates a local acceleration mechanism located on the sunward side of the magnetosphere. The precipitated electron intensity contours as a function of local time are in qualitative agreement with the auroral riometer studies of Basler [1963], for example. This result supports his belief that part of the diurnal variation of ionospheric radio absorption in the auroral region is due to a diurnal variation of corpuscular radiation precipitated into the atmosphere. (Discussion of the enhancement of absorption during daylight hours due to electron photo-detachment processes produced by solar radiation is given by Chapman and Little [1957] and Chapman [1959].) The occurrence of visual aurora [Davis and Dewitt, 1963] has a maximum during local night and is anti-correlated with the downflux of energetic electrons ( $E \geq 40$  keV) in the present study, which displays a broad minimum at local night; the observations of low energy electrons (1 to 10 keV) near the equatorial plane at  $L \gtrsim 8$  on the night side of the magnetosphere [Gringauz et al., 1961, 1963; Freeman, 1964] are correlated in local time with the visual aurora studies.



On the bases of the above local time and latitude surveys of these phenomena it is suggested that the auroral riometer absorption may be at least, in part, attributed to the precipitation of electrons of  $\geq 40$  keV reported here and that the visual aurorae are a distinctly different phenomena, largely associated with the large intensities of low energy electrons (1 to 10 keV) measured by Gringauz and his collaborators and by Freeman on the night side of the magnetosphere. Comprehensive spatial and temporal surveys of these low energy electron intensities throughout the magnetosphere and at its boundary remain a largely unexplored and critical area of experimental interest. The rapid decrease of trapped electron ( $E \geq 40$  keV) intensities for  $L \gtrsim 8$  at high latitudes during local night has a presumptive correspondence to the preliminary results near the equatorial plane with Explorer XIV [Frank, Van Allen, and Macagno, 1963], which also showed a rapid decrease of electron ( $E \geq 40$  keV) intensities at  $L \approx 8.0$  during local night. One measurement [Vakulov et al., 1963] of electrons of similar energies at a geomagnetic latitude of  $\sim 50^\circ$  with the Russian Mars I probe (November 1962) confirms this rapid decrease of intensities on the night side of the earth at an intermediate latitude. The northern limit of detectable trapped electron intensities has been shown here to be  $\Lambda \approx 77^\circ$  ( $L \approx 20$ ) on the noon meridian and  $\Lambda \approx 69^\circ$

( $L \approx 8$ ) on the midnight meridian at low altitudes. Theoretical computations of the motion of electrons of these energies in a model magnetosphere compressed by the solar wind [Hones, 1963] apparently do not yield a latitude displacement of the mirror points of such electrons sufficient in magnitude to account for the observed effect. It may be noted that a comprehensive survey of the distribution of electrons of similar energies at large radial distances and for geomagnetic latitudes of 0 to  $30^\circ$  is now being completed with Explorer XIV. The Explorer XIV study and the present Injun III survey will allow us to display the intensities of trapped electrons ( $E \geq 40$  keV) throughout a major portion of the magnetosphere and allow a critical examination of the magnetospheric models now at our disposal. Further studies now under progress include the investigation of the dependence of the diurnal variations of trapped and of precipitated electrons upon magnetic activity and season.

## REFERENCES

- Akasofu, S.-I., Deformation of magnetic shells during magnetic storms, J. Geophys. Res., 68, 4437-4445, 1963.
- Axford, W. I., and C. O. Hines, A unifying theory of high-latitude geophysical phenomena and geomagnetic storms, Can. J. Phys., 39, 1322, 1961.
- Basler, R. P., Radio wave absorption in the auroral ionosphere, J. Geophys. Res., 68, 4665-4681, 1963.
- Chapman, S., Disturbances in the lower auroral ionosphere, J. Atmospheric Terrest. Phys., 15, 29-37, 1959.
- Chapman, S., and C. G. Little, The nondeviative absorption of high-frequency radio waves in auroral latitudes, J. Atmospheric Terrest. Phys., 10, 20-31, 1957.
- Davis, T. N., and R. N. Dewitt, Twenty-four-hour observations of aurora at the southern auroral zone, J. Geophys. Res., 68, 6237-6241, 1963.
- Frank, L. A., and J. A. Van Allen, Intensity of electrons in the earth's inner radiation zone, J. Geophys. Res., 68, 1203-1207, 1963.
- Frank, L. A., J. A. Van Allen, and E. Macagno, Charged particle observations in the earth's outer magnetosphere, J. Geophys. Res., 68, 3543-3554, 1963.
- Freeman, J. W., The morphology of the electron distribution in the outer radiation zone and near the magnetospheric boundary as observed by Explorer XII, J. Geophys. Res. (1964).

Gringauz, K. I., V. V. Bezrukikh, L. S. Musatov, R. E. Rybchinsky, and S. M. Sheronova, Measurements made in the earth's magnetosphere by means of charged particle traps aboard the Mars I probe, Paper presented at the Fourth International Space Science Symposium (COSPAR), Warsaw, Poland, June 1963.

Gringauz, K. I., V. G. Kurt, V. I. Moroz, and I. S. Shklovskii, Results of observations of charged particles observed out to  $R = 100,000$  km, with the aid of charged-particle traps on Soviet space rockets, Soviet Astronomy (AJ) 4, 680-695, 1961.

Hones, E. W., Motions of charged particles trapped in the earth's magnetosphere, J. Geophys. Res., 68, 1209-1220, 1963.

Little, C. G., and H. Leinbach, Some measurements of high-latitude ionospheric absorption using extraterrestrial radio waves, Proc. IRE, 46, 334-348, 1958.

McIlwain, C. E., Coordinates for mapping the distribution of magnetically trapped particles, J. Geophys. Res., 66, 3681-3692, 1961.

O'Brien, B. J., Lifetimes of outer-zone electrons and their precipitation into the atmosphere, J. Geophys. Res., 67, 3687-3706, 1962.

O'Brien, B. J., A large diurnal variation of the geomagnetically trapped radiation, J. Geophys. Res., 68, 989-996, 1963.

O'Brien, B. J., High-latitude geophysical studies with satellite Injun III, Part 3: Precipitation of electrons into the atmosphere, J. Geophys. Res., 69, 13-43, 1964.

O'Brien, B. J., C. D. Laughlin, and D. A. Gurnett, High-latitude geophysical studies with satellite Injun III, Part 1: Description of the satellite, J. Geophys. Res., 69, 1-12, 1964.

Vakulov, P. V., S. N. Vernov, E. B. Gorchakov, Yu. I. Logachev, A. N. Charakhchyan, T. N. Charakhchyan, and A. E. Chudakov, Investigation of cosmic rays, Paper presented at the Fourth International Space Science Symposium (COSPAR), Warsaw, Poland, June 1963.

## FIGURE CAPTIONS

Figure 1. A summary of local time for Injun III measurements over North America for several values of the shell parameter  $L$ . The local times available during a given month are indicated by the solid bars.

Figure 2. Graphs of the trapped radiation detector response as a function of local time, with  $L$  as a parameter. The diurnal variation begins abruptly between  $L = 7$  and  $8.5$ . Each data point for a given value of  $L$  represents the response of the detector for an individual satellite pass. The various symbols denote ranges of the scalar magnetic field strength  $B$  as follows: for  $L = 4.0$  and  $8.5$ ,  
 $\Delta$  , 0.14-0.21 gauss;  $\circ$ , 0.21-0.25;  $\times$ , 0.25-0.29;  
 $\blacktriangle$  , 0.29-0.35;  $\bullet$ , 0.35-0.44; for  $L = 10$ ,  
 $\times$ , 0.19-0.21;  $\circ$ , 0.21-0.23;  $\blacktriangle$  , 0.23-0.27;  
 $\blacktriangle$  , 0.28-0.50.

Figure 3. A continuation of Figure 2 for higher values of the parameter  $L$ . For  $L = 14$  the symbols denote the following ranges of  $B$ :  $\times$ , 0.19-0.21 gauss;  
 $\circ$ , 0.21-0.23;  $\square$  , 0.23-0.25;  $\blacktriangle$  , 0.25-0.27;  
 $\bullet$ , 0.27-0.29;  $\Delta$  , 0.29-0.46.

Figure 4. The median counting rates of the trapped electron detector as a function of  $L$  for several local times.

Figure 5. A summary of the median omnidirectional intensities of trapped electrons ( $E \geq 40$  keV) measured at low altitudes with Injun III as displayed in a  $L$ -local time coordinate system.

Figure 6. The median omnidirectional intensities of trapped electrons ( $E \geq 40$  keV) measured at low altitudes with Injun III as displayed in a  $\wedge$ -local time coordinate system.

Figure 7. Graphs of the response of the precipitated electron detector as a function of local time and with  $L$  as a parameter. Onset of a large diurnal variation begins between  $L = 7$  and  $8.5$ . The symbols denote various ranges of  $B$  according to the same code as in Figure 2.

Figure 8. A continuation of Figure 7 for higher values of the parameter  $L$ . For a given  $L$  the symbols denote the same ranges of  $B$  as for the trapped radiation detector responses (see Figure 3).

Figure 9. The median counting rates of the precipitated electron detector as a function of  $L$  for several local times.

Figure 10. A summary of the median omnidirectional intensities of electrons ( $E \geq 40$  keV) precipitated into the atmosphere as displayed in a  $L$ -local time coordinate system.

Figure 11. The median omnidirectional intensities of electrons ( $E \geq 40$  keV) precipitated into the atmosphere as displayed in a  $\wedge$ -local time coordinate system.

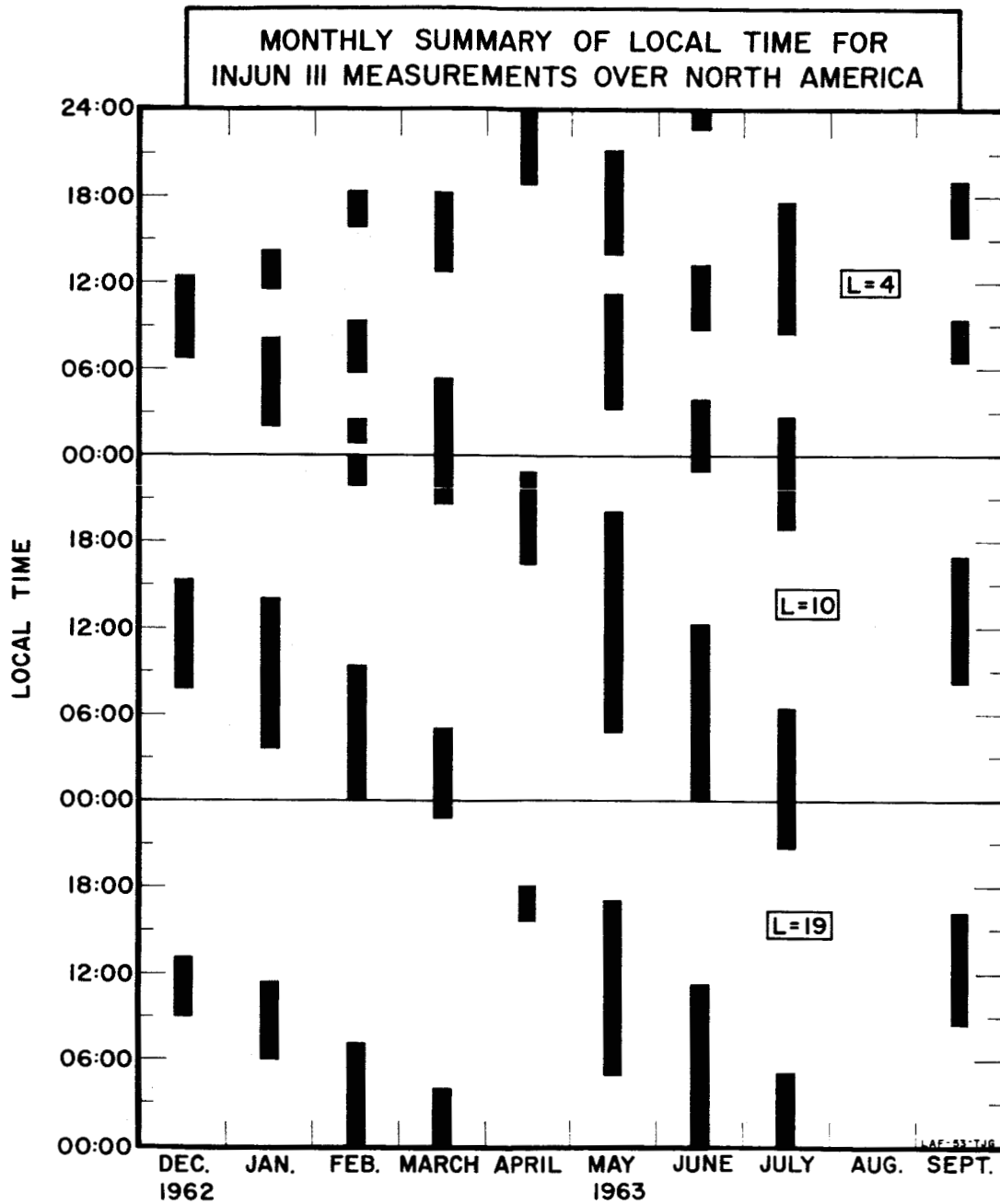


Figure 1



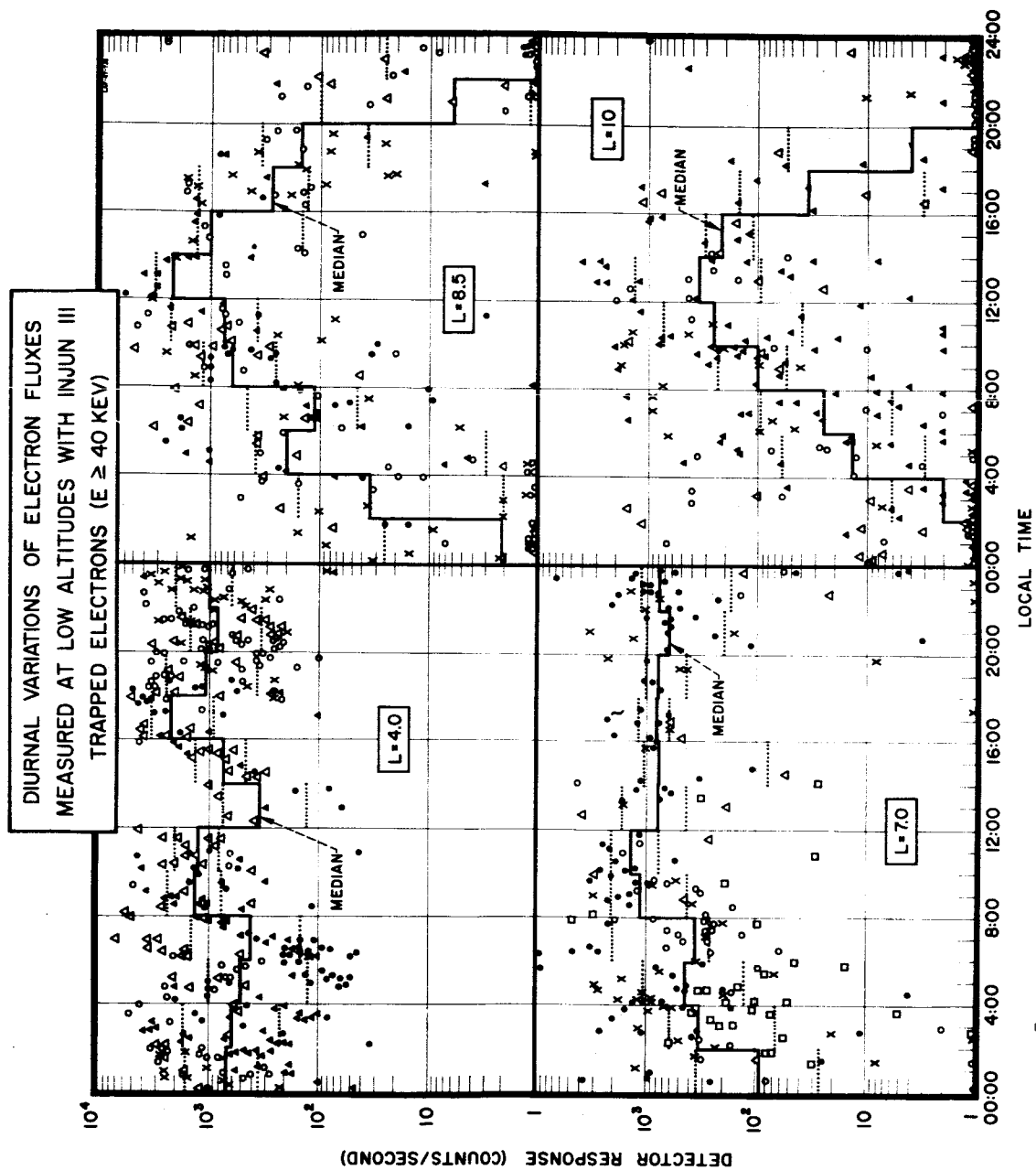


Figure 2

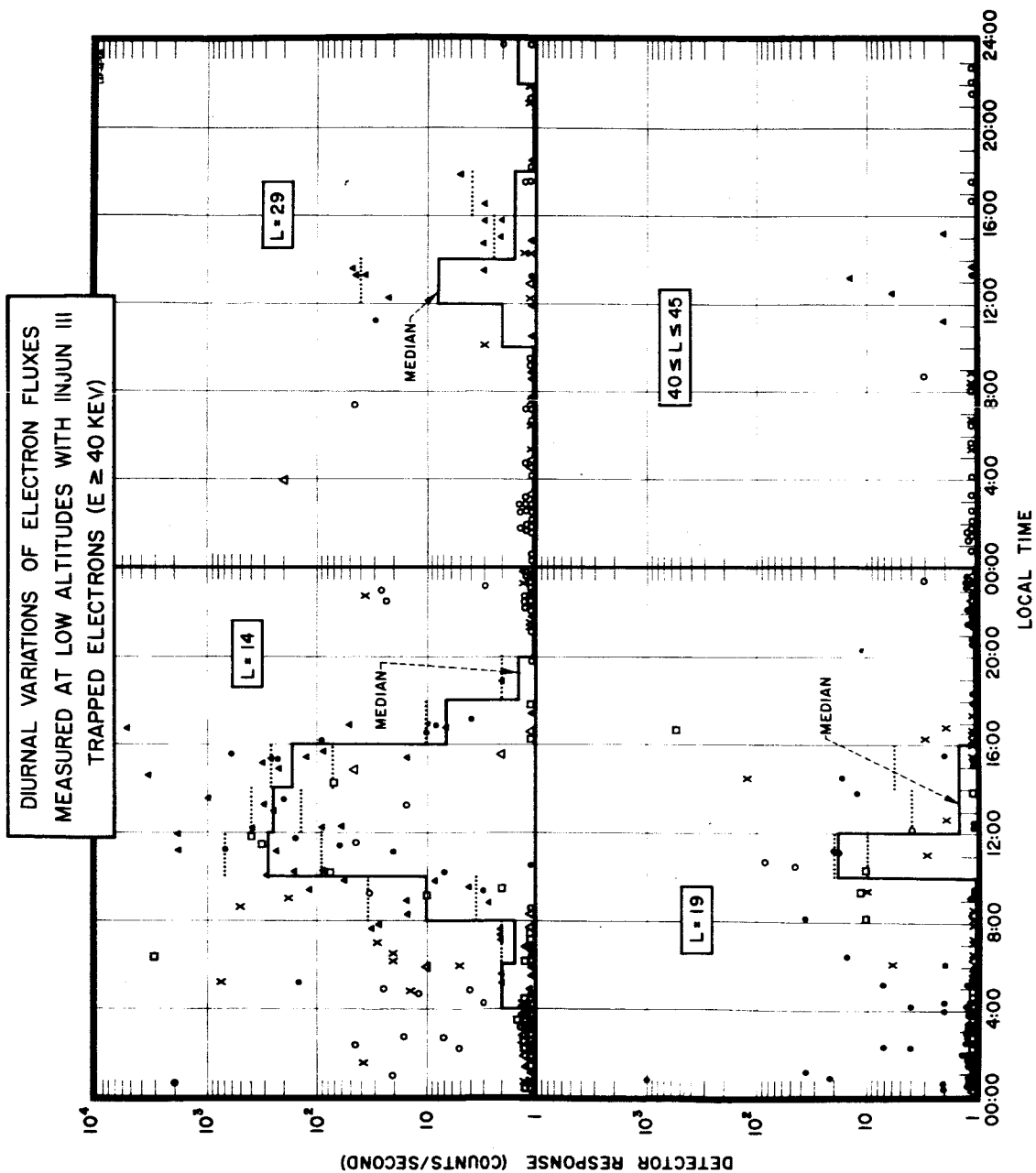


Figure 3

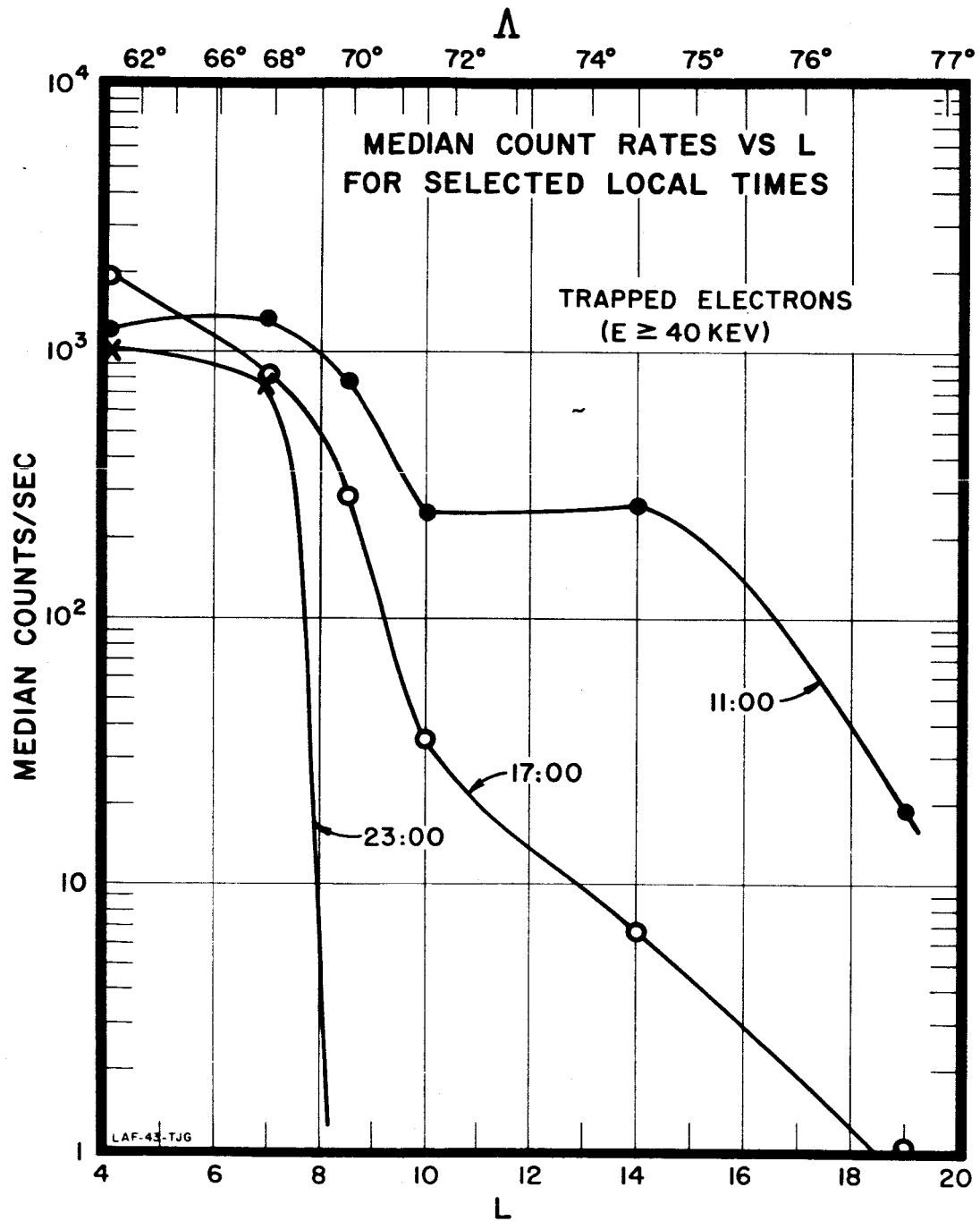
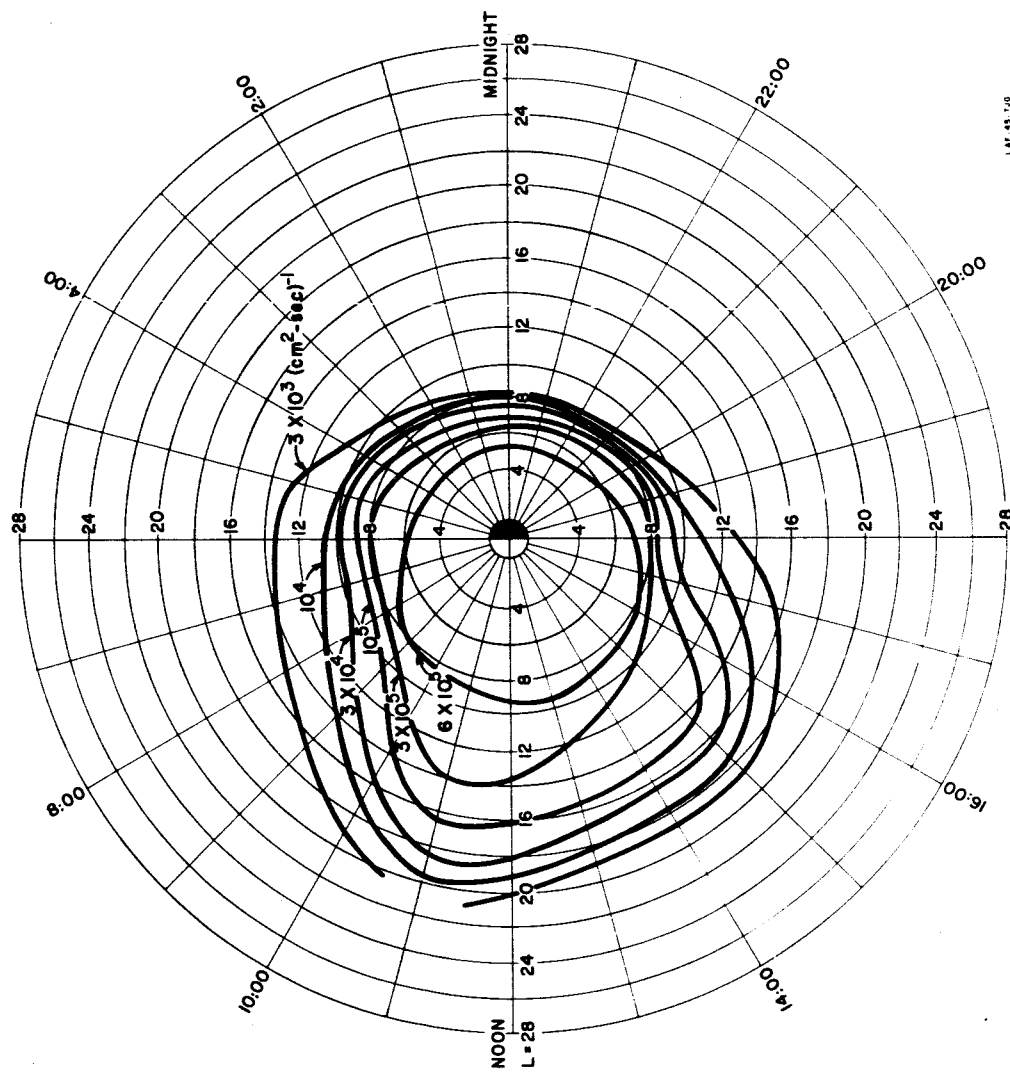


Figure 4

**MEDIAN OMNIDIRECTIONAL INTENSITY OF TRAPPED ELECTRONS ( $E \geq 40$  KEV)  
MEASURED AT LOW ALTITUDES WITH INJUN III**



LAP 45-7-6

**Figure 5**

MEDIAN OMNIDIRECTIONAL INTENSITY OF TRAPPED ELECTRONS ( $E \geq 40\text{KEV}$ )  
MEASURED AT LOW ALTITUDES WITH INJUN III

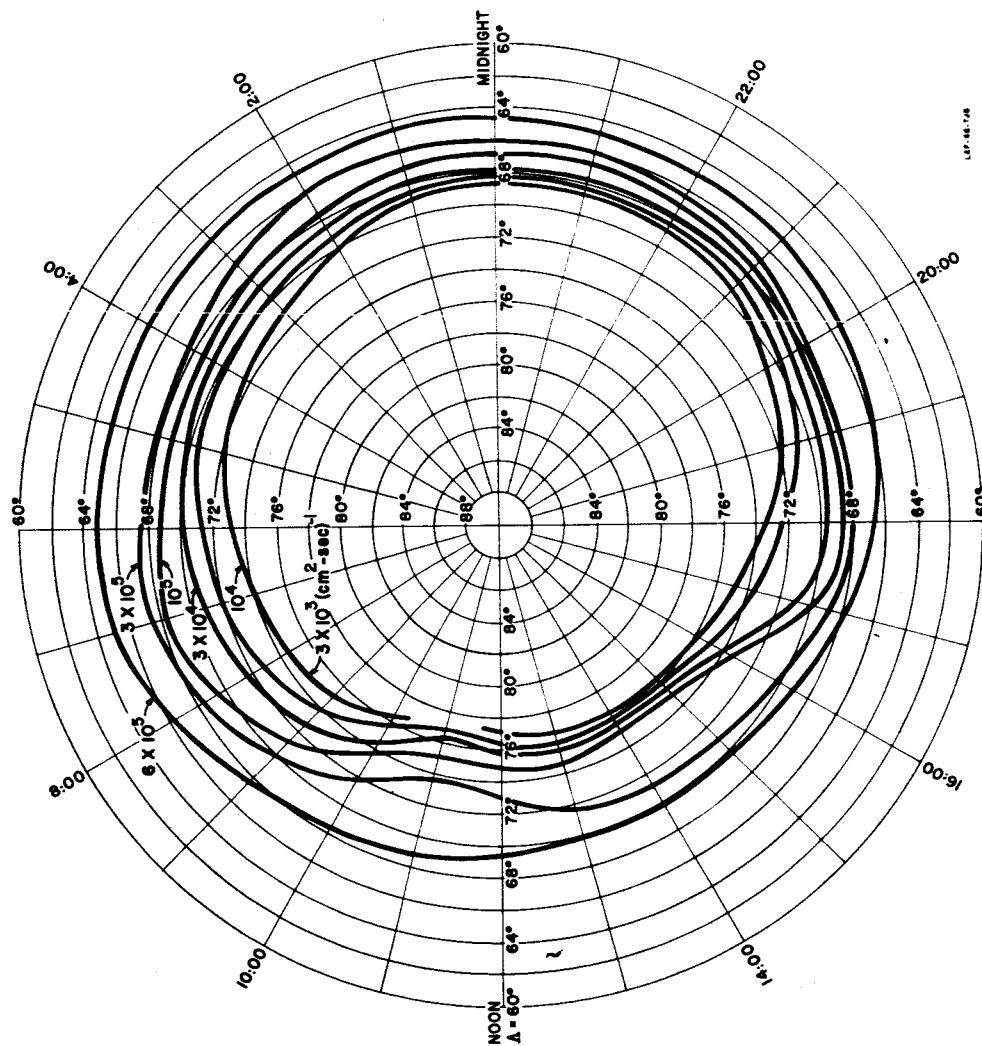


Figure 6

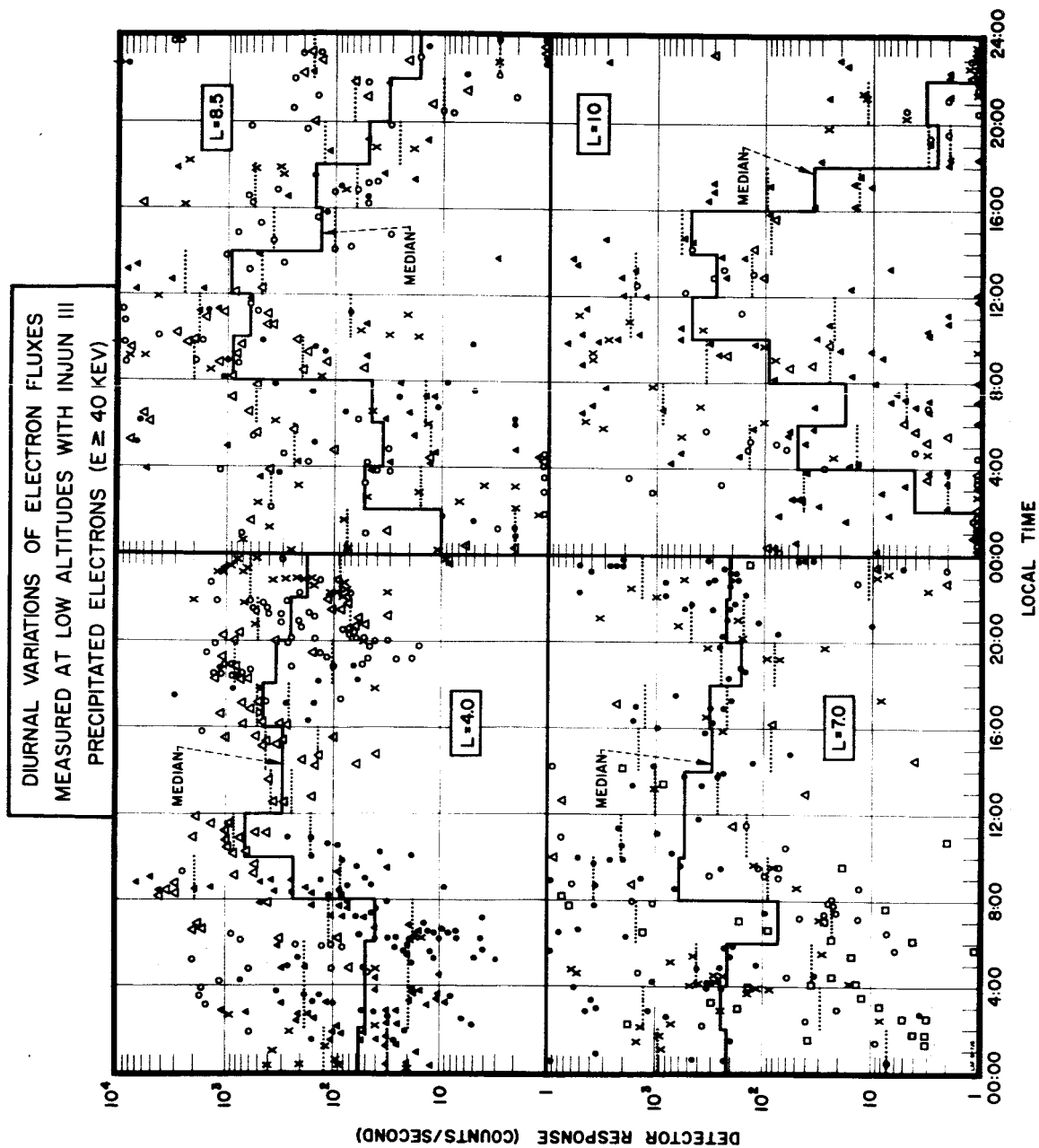


Figure 7

DIURNAL VARIATIONS OF ELECTRON FLUXES  
 MEASURED AT LOW ALTITUDES WITH INJUN III  
 PRECIPITATED ELECTRONS ( $E \geq 40$  KEV)

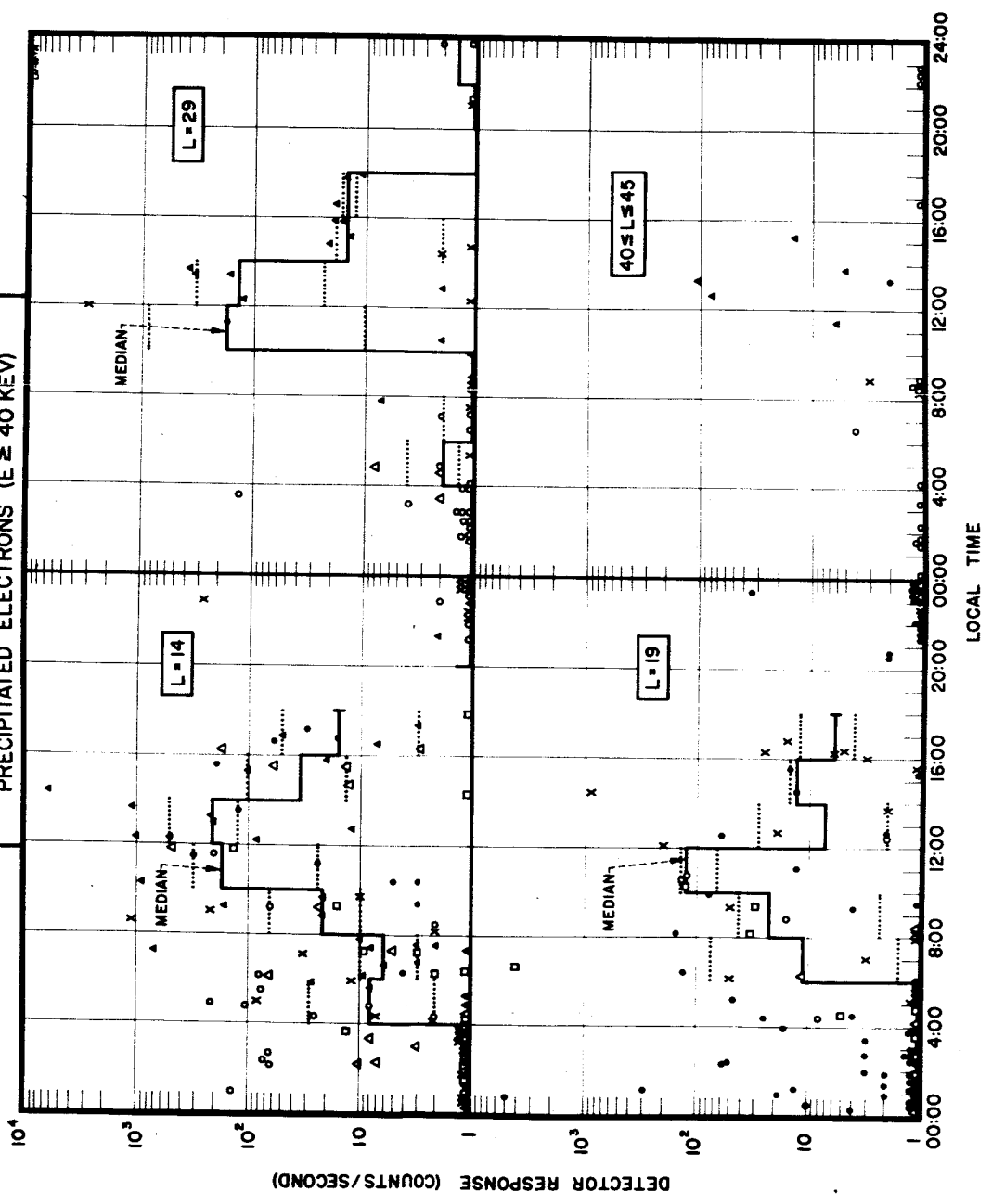


Figure 8

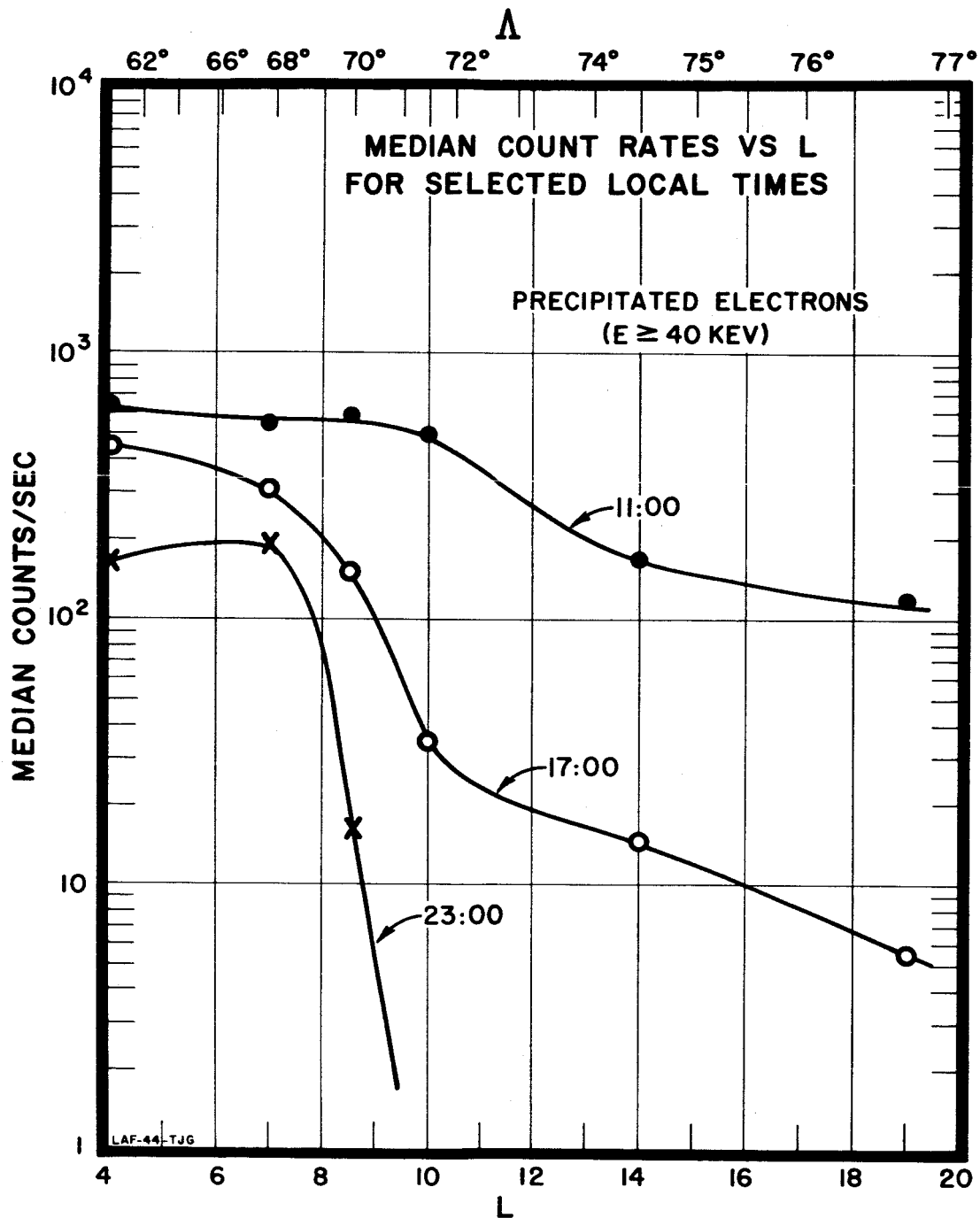
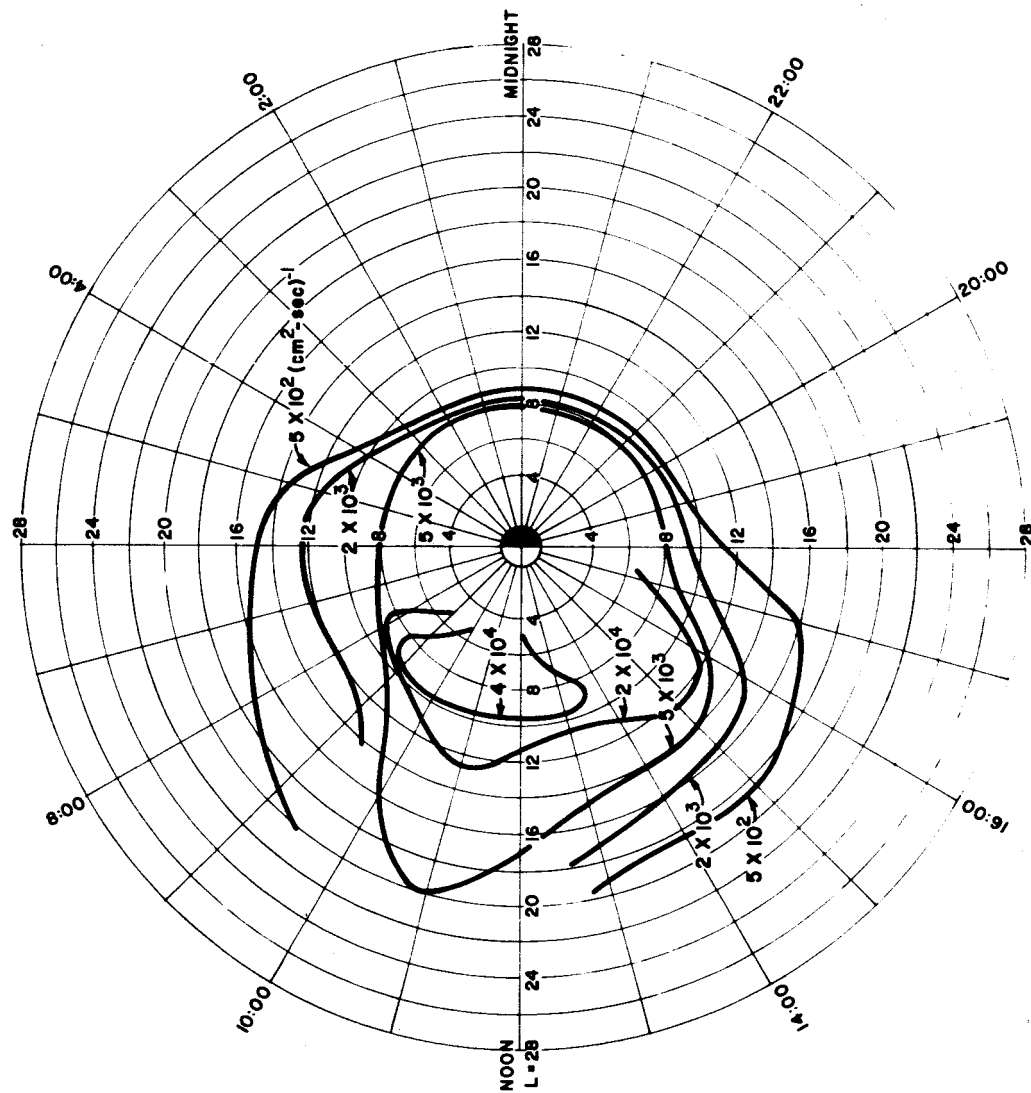


Figure 9



**MEDIAN OMNIDIRECTIONAL INTENSITY OF ELECTRONS ( $E \approx 40$  KEV)  
PRECIPITATED INTO THE EARTH'S UPPER ATMOSPHERE**



**Figure 10**

**MEDIAN OMNIDIRECTIONAL INTENSITY OF ELECTRONS ( $E \geq 40$  KEV)  
PRECIPITATED INTO THE EARTH'S UPPER ATMOSPHERE**

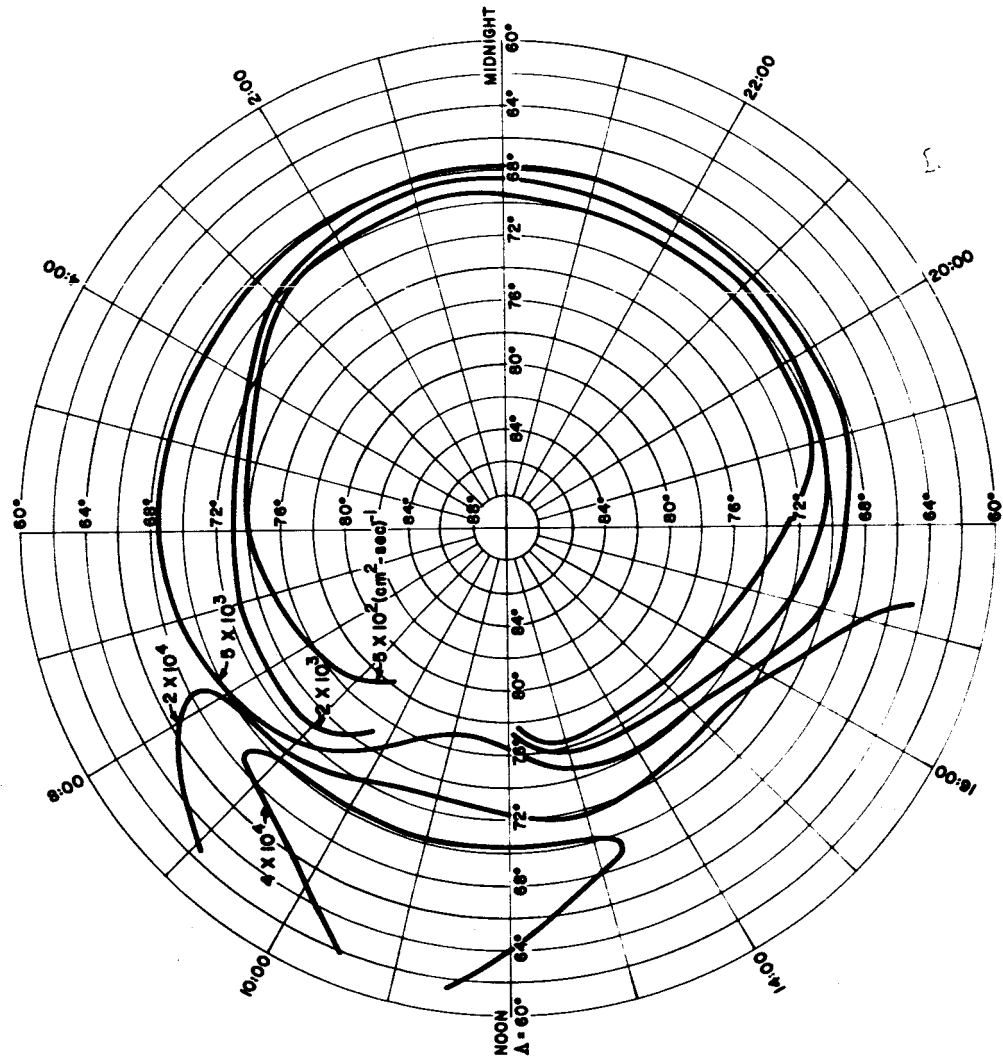


**Figure 11**